Supporting Information for

Deterministic Assembly of 3D Suspended Nanowire Structures

Hongyan Gao[1], Bing Yin[1], Siyu Wu[1], Xiaomeng Liu,[1] Tianda Fu,[1] Cheng Zhang,[2] Jian Lin,[2] Jun Yao[1,3],*

---

1. Department of Electrical Computer and Engineering, University of Massachusetts, Amherst, MA, USA.

2. Department of Mechanical & Aerospace Engineering, University of Missouri, Columbia, MO, USA.

3. Institute for Applied Life Sciences (IALS), University of Massachusetts, Amherst, MA, USA.

This PDF file includes:

Materials and Methods
Supplementary Figures 1 to 5
References

Materials and Methods

Silicon (Si) nanowire synthesis.

The Si nanowires were grown by a nanocluster-catalysed vapour–liquid–solid method described previously.[1-3] Briefly, the growth substrate, a Si substrate cover with 600 nm thermal SiO_2 (Nova Electronic Mater.), was cleaned by oxygen plasma (50 W, 1 min). The cleaned substrate was treated with poly-L-lysine solution (0.1%, Ted Pella) for 5 min, and then rinsed thoroughly with deionized water. Gold nanoparticles with an average diameter of 20 nm (Ted Pella) were then dispersed on the growth substrate. The growth was carried out at 442 °C under a constant pressure of 40 torr, with SiH_4 (2.5 s.c.c.m.), diluted B_2H_6 (100 ppm in He, 3 s.c.c.m.) and H_2 (60 s.c.c.m.) as reactant, doping and carrier gases, respectively. The growth time was 90 min, producing an average nanowire length ~60 μm.

Deterministic combing.

The deterministic combing followed a previously developed process.[2,4] Resist (Microposit S1805, 1:4 (vol:vol) diluted in Microposit Thinner-P) at a thickness of 50 nm was spin-coated on the target substrate (SiO_2/Si). To define the anchoring window (*i.e.*, 2×20 μm² exposed SiO_2 surface), standard photolithography was performed, followed by development (40 s in Microposit MF-CD-26), a short deionized-water rinse (10 s), and nitrogen drying. Because the tetramethylammonium hydroxide (TMAH) component in the developer is considered to simultaneously functionalize the target-substrate (SiO_2/Si) surface to be highly hydrophilic and hence attractive to Si nanowires, a sufficient development time (*e.g.*, >20 s) was necessary. The target substrate with defined anchoring windows was then immediately mounted onto a movable stage controlled by a micromanipulator.[2] Approximately 40 μl mineral oil (#330760, Sigma-Aldrich) was drop-cast onto the target substrate as the lubricant. The nanowire growth substrate (1.2×1 cm²) was then brought into contact with the target substrate with a constant pressure ~5 N·cm⁻². During combing, the target substrate was moved by the micromanipulator at a constant velocity ~5 mm·min⁻² with respect to the fixed growth substrate. The oil lubricant was removed gently by flowing drops of octane over the substrate followed by gentle drying with nitrogen. The underlying resist layer was removed by oxygen plasma (50 W, 10 min). Alternatively, acetone vapor may be employed to remove the resist layer without perturbing assembled nanowire position and alignment.[4]

Definition of microbars.

The SU-8 microbars were fabricated by electron-beam lithography (EBL). The SU-8 resist (Microchem) was spin-coated on the target (SiO_2/Si) substrate. Different SU-8 compositions and spin-coating rates were used to yield different thicknesses involved in this research. The resist was then prebaked (95 °C), followed by EBL exposure, post-bake (95 °C) and development in SU-8 developer (Microchem). Processing details related to different SU-8 thicknesses involved in this research were

summarized in the following table. The defined microbars by above steps were further hard-baked (180 °C, 10 min). Before the assembly, SU-8 microbars were cleaned by acetone, isopropanol and oxygen-plasma treatment (*e.g.*, 50 W, 30 s).

Table S1. SU-8 processing details

Height of SU-8 microbar (μm)	SU-8 composition	Spin-coating rate (rpm)	Pre-bake (95 °C) time (min)	EBL exposure dose ($\mu C/cm^2$)	Post-bake (95 °C) time (min)	Development time (sec)
0.4	SU-8 2000.5	3000	1	0.7	1	30
1.0	SU-8 2002: 2000.5 = 2:1 (*v:v*)	2000	1	0.9	2	30
1.4	SU-8 2002	3000	1	0.95	2	40
2.1	SU-8 2002	1000	1	1.0	2	50
6.0	SU-8 2005	2000	2	1.5	3	60

Transfer process.

The microbar arrays on the target substrate were defined by standard EBL. Briefly, SU-8 resist (Microchem) of different thicknesses (*e.g.*, 0.4 – 6.0 μm) was spin-coated on the target (SiO_2/Si) substrate. EBL was employed to expose/crosslink the size of a microbar (*e.g.*, 0.8×10 μm^2), followed by development and hard bake (180 C°, 10 min). Alternatively, photolithography was also employed to define the SU-8 microbar arrays (for making the mechanical sensor devices). Due to resolution limit, SU-8 microbars with a width of 2 μm were achieved in photolithography. The peeling-off and transferring of assembled planar nanowires on to the microbars are described with details in **Supplementary Fig. S1**.

Device fabrication.

Photolithography was carried out to define the electronic contacts to the assembled 3D nanowire structures. Specifically, to avoid perturbing assembled 3D nanowire structure by centrifugal force, a spin-coat rate of 1000 RPM was employed to coat the first resist layer (Microchem LOR 3A). The second resist layer (Microchem S1805) was spin-coated at 4000 RPM. After exposure and development, the exposed nanowire region in the contact area was cleaned by oxygen plasma (50 W, 30 s) and a quick treatment (3 s) in buffered oxide etch (7:1; JT Baker) to remove surface oxide. Immediately, the sample was put into an electron beam evaporator for metal deposition (Cr/Au = 3/50 nm), followed by standard lift-off process. A ~1 mm thick polydimethylsiloxane (PDMS; Sylgard 184, 10:1 mix ratio; Dow Corning) layer was cured over the device chip to serve as the encapsulating elastomer for pressure load. A softer version of PDMS (70% crosslink PDMS with 20:1 mix ratio and 30% methyl-terminated linear PDMS) was also used as the encapsulating elastomer. Wire bonding was used to connect the fan-out electrodes on the chip to a printed circuit board (PCB) that can further connect to external recording system.

Electrical measurements.

The electrical measurements were performed in ambient environment. The nanowire conductance was measured by an Agilent 4155C semiconductor parameter analyzer, with the signal acquired by a computer running Easyexpert software. The pressure on the PDMS elastomer was applied by using a mechanical testing stage (ESM303; Mark-10 Inc.) equipped with a force gauge (M7-5; Mark-10 Inc.) and computerized control system.

Mechanical modelling and calculation of *piezoresistive* properties in Si devices.

The 3D nanowire device we made had an electrode spacing ~21.5 μm. The SU-8 microbar had dimensions of 1.4 μm high, 2 μm wide and 20 μm long. Based on SEM imaging, the average span of the nanowire suspension ~5.3 μm (Fig. 3g(iii)). Above geometric parameters (including tracing the geometric shape of the nanowire) were used for the simulation of strain profile in the nanowire by finite element analysis (COMSOL 4.3). We also assumed that the planar portion of the Si nanowire on substrate and the apex portion in contact with the SU-8 microbar were fixed due to strong *van der Waals* forces. Then the nanowire device with the obtained geometry was embedded in the central region of a PDMS matrix (22×22 μm^2, 2 μm thick) with uniform pressure applied from the top. The elastic modulus of the SU-8, PDMS, and Si nanowire was taken as 2.0 GPa, 2.6 MPa, and 187 GPa, respectively.[5,6]

Analyses of the device gauge factor, *piezoresistance* coefficient, and force sensitivity were carried out as follows. First, the pressure sensitivity (η), defined as the relative conductance change ($\Delta G/G$) per applied pressure (P), was obtained from a linear fit of the $\Delta G/G$ data (Fig. 4b):

$$\eta = (\Delta G/G)/P = (5.0 \pm 0.76) \times 10^{-5} \text{ kP}^{-1} \tag{1}$$

Second, from the simulation (Fig. 4c), the strain sensitivity (k), defined as a net strain change ($\Delta \varepsilon$) per applied pressure (P) in the nanowire, was used to obtain the strain sensitivity (k):

$$k = \Delta \varepsilon / P = -5.42 \times 10^{-8} \text{ kPa}^{-1} \tag{2}$$

From equations (1) and (2), we obtained the average gauge factor $\bar{g}$ of devices as:

$$\bar{g} = (\overline{\Delta R/R})/\Delta \varepsilon = -(\overline{\Delta G/G})/\Delta \varepsilon = -\bar{\eta}/k = 920 \pm 140 \tag{3}$$

The axial stress induced in the nanowire is $X = \Delta \varepsilon \times E$, where E is the elastic modulus of material. The corresponding average *piezoresistance* coefficient, $\overline{\pi_L}$, defined as the relative conductance change ($\Delta G/G$) per axial stress, X, was obtained as:

$$\overline{\pi_L} = (\overline{\Delta G/G})/X = (\overline{\Delta G/G})/(\Delta \varepsilon \times E) = -\bar{g}/E = -(490 \pm 75) \times 10^{-11} \text{ Pa}^{-1} \tag{4}$$

The value in the average piezoresistance coefficient is substantially larger than the typical values from bulk Si (-17 to -94×10^{-11} Pa^{-1}) and consistent with the giant piezoresistance effect observed in Si nanowires.[7] We assume that the piezoresistance coefficient is largely constant in the low-strain regime (<0.3%) of these experiments.[7] Therefore, a net strain $\Delta \varepsilon$ value can be used for calculation of gauge factor and piezoresistance coefficient.

Last, as the equivalent force exerted along the axis of nanowire, F, is the product of axial stress (X) and cross-section area (A), with the cross-section area A further related to the diameter of nanowire ($d\sim30$ nm) as $A = \pi d^2/4$. At the loading pressure of 4 kPa, the average net strain $\Delta\varepsilon$ is $\sim2.17\times10^{-7}$ (Fig. 4c). So we obtained:

$$F = X \times A = \Delta\varepsilon \times E \times (\pi d^2/4) = 29 \text{ pN} \tag{5}$$
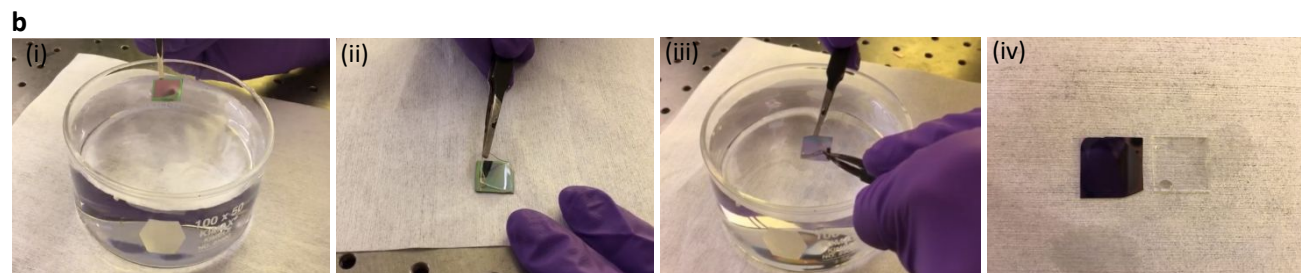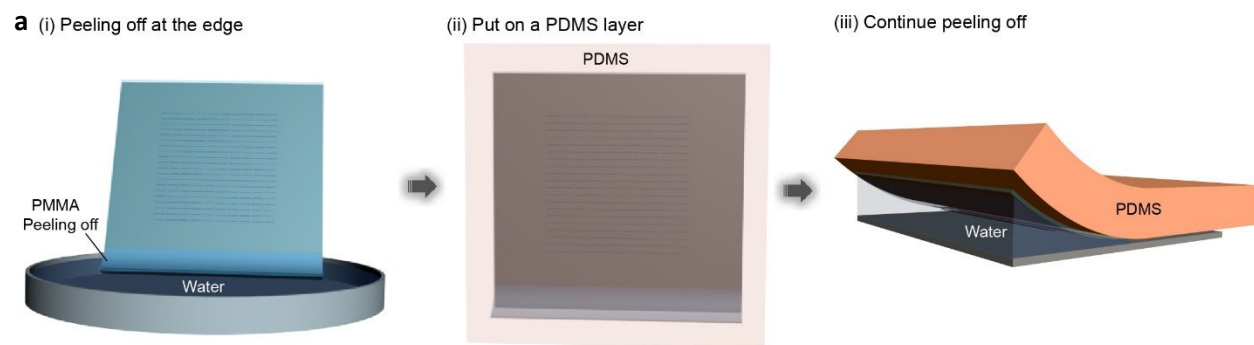
Figure S1. a, Schematics of the peel-off process. After the planar nanowire assembly and cleaning, the substrate was treated with oxygen plasma (50 W, 30 s). The oxygen plasma was to increase the surface hydrophilicity to facilitate interfacial water intercalation during peel-off process. After the treatment, a thin layer of PMMA (Microchem 950 PMMA C2) with a thickness ~100 nm was spin-coated on the substrate and baked (100 °C, 2 min). (i) The edge of the PMMA-coated substrate was then dipped into a water surface, during which the the PMMA-substrate interface was intercalated by water molecules and yielded PMMA peeling off at the edge.[8] (ii) Without further peeling off in water, the substrate was then taken out and covered by a PDMS layer (~ 1 mm thick) that was slightly larger than the sample size. (iii) By gradual peeling off in the PDMS layer, the water at the PMMA-substrate interface penetrated deeper to sustain a continuing delamination between the PMMA and substrate. Eventually, the PMMA layer, with embedded nanowires, was completely peeled off from the substrate and attached to the PDMS handle layer. **b**, The actual processes of (i) peeling off the PMMA edge, (ii) placing a PDMS stamp, (iii) continuing peeling and (iv) finishing.
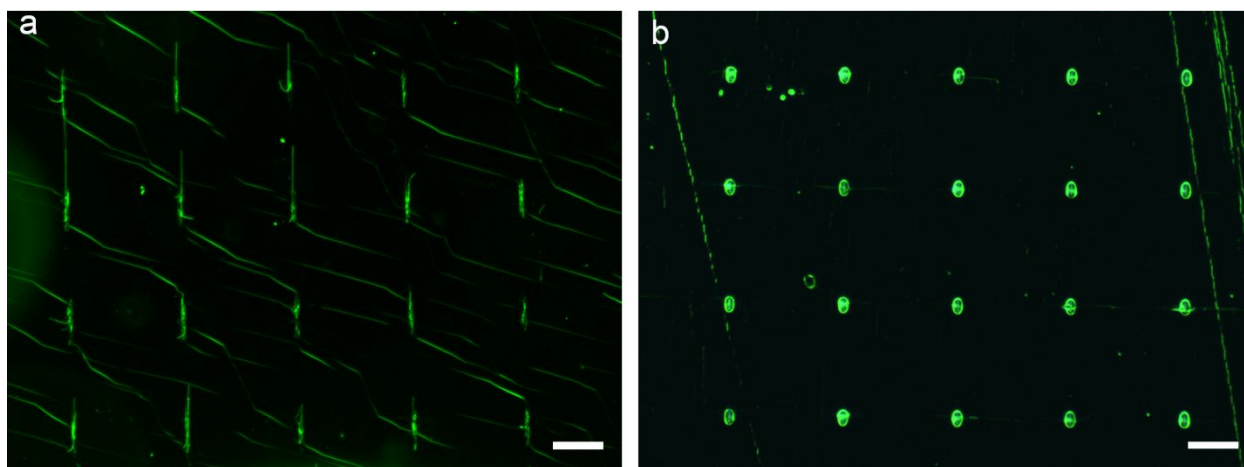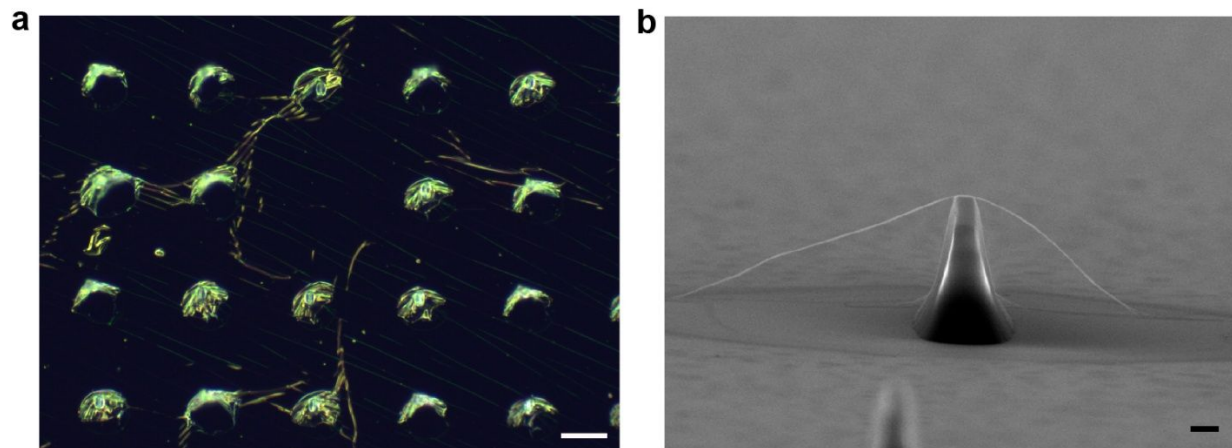
Figure S2. **a**, Dark-field optical image of peeled-off nanowire arrays embedded in the PMMA carrier layer, which was further attached on a PDMS soft stamp. Scale bar, 50 µm. **b**, Dark-field optical image of a transferred PMMA layer laying on the SU-8 microbar arrays. Uniform microscale-tent features, which eventually defined the nanowire spanning configuration, were formed around the SU-8 microbars. Scale bar, 50 µm.
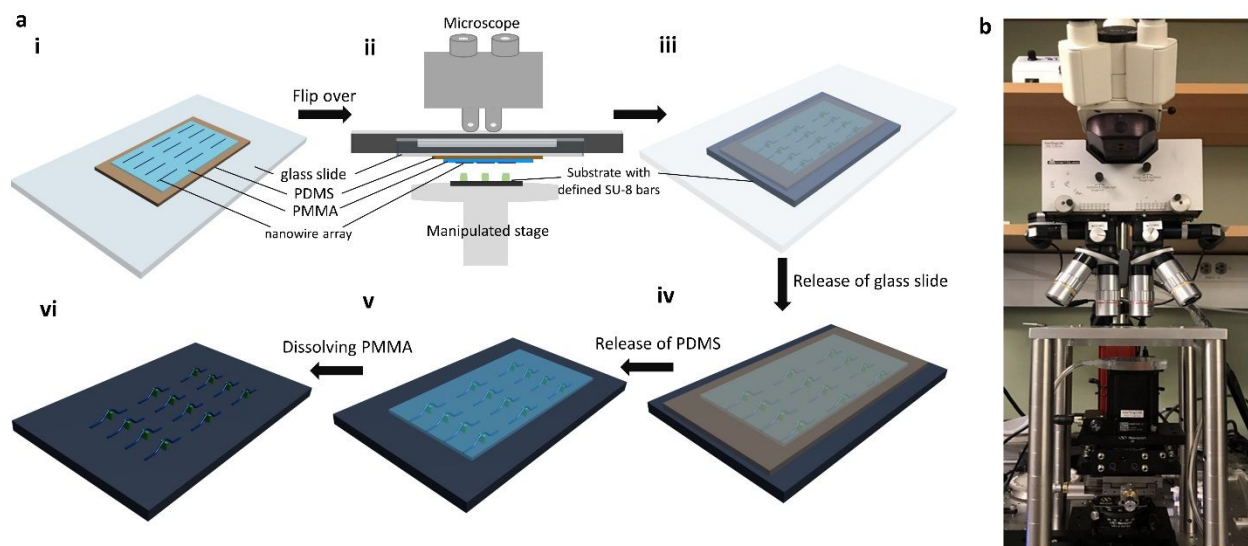
Figure S3. Aligned transfer process. **a**, (i) The PDMS soft stamp, which is attached with the PMMA layer containing the peeled-off nanowires, is attached on a glass slide by using a thermal-release tape (Revalpha, Nitto Denko Corp.). (ii) The (flip-over) glass slide is then mounted (by vacuum) on a fixed (top) stage of a home-built alignment system. The target substrate, with defined SU-8 microbar arrays, is mounted on the movable (bottom) stage controlled by micromanipulators. The transparency in the transfer substrate (*e.g.*, glass/PDMS/PMMA) allows the optical alignment between the assembled nanowire arrays and SU-8 microbar arrays. Once aligned, the (bottom) target substrate is raised by a micromanipulator to contact the (top) transfer substrate. (iii) The transfer and target substrates, attached together by *van der Waals* force, are unmounted from the alignment system. (iv) The glass slide is then thermally released from the PDMS soft stamp at 100 °C. (v) The PDMS stamp is further peeled off from the substrate, assisted by a thermal treatment at 100 °C for 5 min. (vi) Finally, the PMMA layer is removed in acetone solution for 10 min, yielding suspended nanowires over the microbars. (**b**) Optical image of the home-built alignment system for the transfer process.

Figure S4. a, Dark-field optical image of transferred PMMA layer laying on arrays of SU-8 microbars having a height of ~6 μm. Film rupture was observed. Scale bar, 30 μm. **b**, As long as the PMMA layer was unbroken in some microbar region, the nanowire could still bridge over the microbar to form suspended structure, although the large tension in the PMMA layer could yield less symmetry in the two arms. Scale bar, 1 μm.
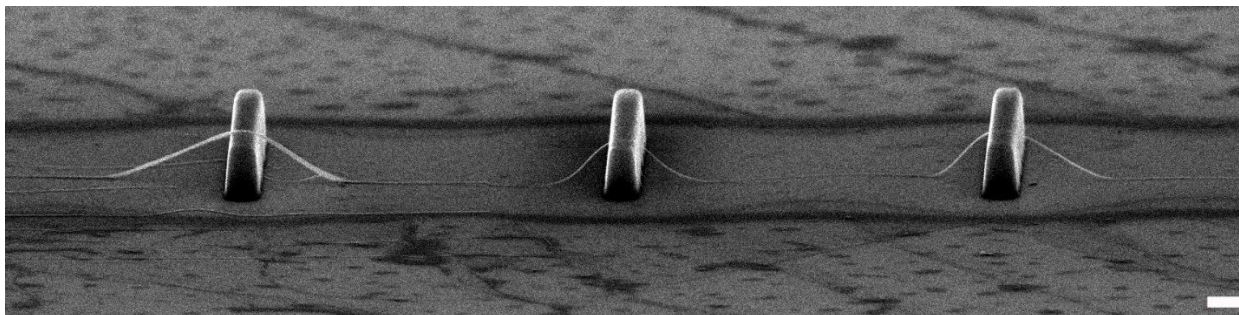
Figure S5. Assembled nanowire structure over three microbars that were 10 µm spaced. The nanowire damped to the substrate, which was due to the collapse of the PMMA carrier layer during the transfer. Note that Si nanowire has enhanced fracture limit (*e.g.*, >20%) at nanoscale.[5,9] Consequently, the damping did not necessarily yield breakage in the nanowire. Scale bar, 1 µm.

References

1. Cui, Y.; Zhong, Z.; Wang, D.; Wang, W. U.; Lieber, C. M. *Nano Lett.* **2003**, 3, 149–152.
2. Yao, J.; Yan, H.; Lieber, C.M. *Nat. Nanotechnol.* **2013**, 8, 329-335.
3. Zhao, Y.; Yao, J.; Xu, L.; Mankin, M.; Zhu, Y.; Wu, H.; Mai, L.; Zhang, Q.; Lieber, C.M. *Nano Lett.* **2016**, 16, 2644-2650.
4. Yao, J.; Yan, H.; Das, S.; Klemic, J.; Ellenbogen J.; Lieber, C.M. *Proc. Natl. Acad. Sci. USA* **2014**, 111, 2431-2435.
5. Zhu,Y.; Xu, F.; Qin, Q.; Fung, W. Y.; Lu, W. *Nano Lett.*, **2009**, 9, 3934–3939.
6. Wang, Z.; Volinsky, A. A.; Gallant, N. D. *J. Appl. Polym. Sci.* **2014**, 131, 41050.
7. He, R.; Yang, P. *Nat. Nanotechnol.* **2006**, 1, 42-46.
8. Li, H.; Wu, J.; Huang, X.; Yin, Z.; Liu, J.; Zhang, H. *ACS Nano*, **2014**, 8, 6563–6570.
9. Tang,D.-M.; Ren, C.-L.; Wang, M.-S.; Wei, X.; Kawamoto, N.; Liu, C.; Bando, Y.; Mitome, M.; Fukata, N.; Golberg, D. *Nano Lett.*, **2012**, 12, 1898–1904.